Macromolecules
ARTICLE

Macromolecules **2010**, *43*, 9945–9956 **9945**
DOI: 10.1021/ma101439f

Precise Synthesis and Physicochemical Properties of High-Density Polymer Brushes designed with Poly(*N*-isopropylacrylamide)

Hiromasa Suzuki,[†] Huda Muhammad Nurul,[†] Takahiro Seki,[†] Taisuke Kawamoto,[‡] Hisashi Haga,[‡] Kazushige Kawabata,[‡] and Yukikazu Takeoka*,[†]

[†]*Department of Molecular Design & Engineering, Nagoya University, Furo-cho, Chikusa-ku, Nagoya, 464-8603, Japan, and* [‡]*Division of Biological Sciences, Graduate School of Science, Hokkaido University, Sapporo 060-0810, Japan*

Received June 29, 2010; Revised Manuscript Received October 24, 2010

ABSTRACT: A high-density polymer brush of poly(*N*-isopropylacrylamide) (PNIPA) was precisely prepared following carefully selected procedures, which included selecting the underlying substrate, preparing its surface, and grafting PNIPA on the substrate. As a result, the graft density and the dried thickness of the brush reached more than 0.5 chains/nm^2 and 200 nm, respectively, for the best combination of each procedure. This high-density polymer brush showed gradual collapse with increasing temperature in water, which must be attributed to both the low swelling and the low shrinking abilities of the brush that result from the physically constrained state of the polymers. The contact angle of the air bubbles underneath the high-density polymer brush also gradually decreased up to around 25 °C in water with increasing temperature, which indicates that the hydrophilicity of the surface decreases as it does in typical PNIPA-grafted membranes and gels. Starting at the lower critical solution temperature of free PNIPA in water, approximately 32 °C, the value of the contact angle started to increase dramatically, and it became constant when the solution temperature exceeded 40 °C. Ultimately, the surface exhibited a mostly hydrophilic nature at higher temperatures. The temperature-dependent contact angles can be interpreted by assuming that the terminally chlorinated alkyl groups of the elongated PNIPAs can be positioned on the surfaces or hidden in the vicinity of the membranes, depending on the temperature of the solution.

Introduction

Stimuli-sensitive polymers have received constant attention as building blocks for the fabrication of smart soft materials[1−3] with various forms, such as dispersed colloidal aggregations,[4,5] grafted membranes,[6] and gels.[7,8] When exposed to small alterations in the environment, such as temperature, pH, solvent composition, and ionic strength, smart soft materials can dramatically transform their shape and size. (The term "smart" here means that the soft materials are sensitive to changes in the environment.) Smart soft materials have received a great deal of interest for their manifold applications, including drug delivery systems,[9−13] sensors,[14] on−off switches,[15] artificial muscles,[16] and catalysts.[17]

The anticipated physicochemical properties of smart soft materials in many cases conform to the inherent physicochemical properties of the stimuli-sensitive polymers used. For example, if a certain polymer is sensitive to environmental temperature and exhibits a coil−globule transition at a given temperature, the gel composed of this thermo-sensitive polymer is expected to show a drastic volume change at a similar transition temperature.[18] However, there can be a difference between the two due to intermolecular cooperation between the polymers in the gel. Cooperation occurs mainly as a result of the enhancement of interactions between the polymers. Soft materials that are less affected by interactions, such as a weakly cross-linked polymer gel, may exhibit slightly different properties, but the variances are predictable. As a result of recent advancements in synthetic technology, however, highly ordered soft materials can be fabricated, and their physicochemical properties are strongly influenced by molecular interactions.[19−21] In particular, we are interested in recent progress in controlled or living radical polymerizations,[22−25] which can be applied in various smart soft materials with ordered architectures. Such organized smart soft materials are complex, which is unexpected given the properties of the component polymer in the diluted solution[26] and have potential in both basic and applied research.

In this work, we present the precise preparation of a high-density brush of poly(*N*-isopropylacrylamide) (PNIPA) by atom transfer radical polymerization (ATRP) and its physicochemical properties, which are distinct from those of past sparsely grafted PNIPA membranes and roughly prepared PNIPA brushes. PNIPA is a representative thermo-sensitive polymer that exhibits a lower critical solution temperature (LCST) in water with a temperature around 32 °C. This thermo-sensitive behavior has been modified for a variety of purposes. For example, when using a PNIPA-grafted membrane to control cell adhesion,[27] the change in the wettability of the outer surface of the membrane is critical to the expected physicochemical properties of this membrane. For the preparation of cell sheets, the surface must be hydrophobic around the cultivation temperature, i.e., 37 °C, and hydrophilic below the LCST. As a result, the cell sheets cultured at 37 °C that are useful for tissue engineering are safely isolated from the membranes below the LCST. Such a thermo-sensitive behavior of PNIPA-grafted membranes has been reported in many studies.[12,27−31] This behavior can be easily expected for the soft materials that are less affected by intermolecular interactions. In case of soft materials with highly ordered structure, however, we cannot easily anticipate the property from the behavior of linear PNIPA in water. If a high-density brush of PNIPA were obtained, it would reveal more complex behavior due to the presence of intermolecular interactions. Despite the expectation, in many past results, grafted PNIPA membranes identified as high-density brushes reveal straightforward thermo-sensitive

*To whom correspondence should be addressed. E-mail: ytakeoka@apchem.nagoya-u.ac.jp..

Published on Web 11/10/2010

property reflecting the PNIPA's behavior in water. So far as we know, we believe that inappropriate methods were selected for making the high-density brushes of PNIPA. It has only recently been seriously considered that we have to choose the appropriate surface conditions for attaching PNIPA to one end and the preparatory method to form grafted PNIPA for making a real high-density brush of PNIPA. Indeed, our precisely prepared high-density brush composed of highly ordered PNIPA exhibits an unexpected change, especially in the wettability results, due to temperature change: whereas the hydrophilicity of the surface decreased with an increase in temperature from 10 to 25 °C, the surface regained hydrophilicity with a further increase in temperature and became mostly hydrophilic at higher temperatures. Judging from the important parameters controlling wettability and our experimental results, this temperature-dependent contact angle may be understood by assuming that the terminally chlorinated alkyl groups of the elongated PNIPAs can be positioned on the surfaces or hidden in the vicinity of the membranes, depending on the temperature. Here, we describe the preparation procedure and the various physicochemical properties of the high-density brush composed of PNIPA and discuss the cause of the unexpected surface wettability change of the brush.

Experimental Section

Materials. Ethyl 2-chloropropionate (ECP) (Wako Pure Chemical Industries, Ltd., 96%), copper(I) chloride (beads, 99.99%), and dimethyl sulfoxide (DMSO) (anhydrous, 99.9%), 10% HCl aqueous solution (Wako Pure Chemical Industries, Ltd.), platinum-(0)−1,3-divinyl-1, 1,3,3-tetramethyldisiloxane 0.10 M in xylene (Karstedt Catalyst) (Sigma-Aldrich Co.), and 0.2 M ethylenediaminetetraacetic acid disodium solution (EDTA solution) (Kishida Chemical Co, Ltd.) were used as supplied. Tetrahydrofuran (THF) (Kishida Chemical Co, Ltd.) and toluene (Kishida Chemical Co, Ltd.) were distilled from calcium hydride. NIPA (Kohjin) was recrystallized twice from toluene-hexane mixed solvent and dried under a vacuum prior to use. Tris[2-(dimethylamino)ethyl]amine (Me_6TREN) was obtained as a gift from Mitsubishi Chemical Co. and distilled at 110 °C with 5 mmHg. Deuterated solvents, dimethyl sulfoxide-d_6 (DMSO-*d*) and deuterium oxide (D_2O), for ^{1}H NMR and FT-IR analyses, were used as received. Water was purified using a Direct-Q UV water purification system (Millipore Corp.) and used in all experiments. All other chemicals used in this study were purchased at the highest purity and used as received. A silicon wafer with a crystalline orientation of 100 and one polished side was purchased from Toshiba Semiconductor Company.

Sample Synthesis. *Preparation of* [*11-(2-Chloro)propionyloxy*]*undecyldimethylchlorosilane* (*CPU−dMCS*) *as Surface-Attachable ATRP Initiator*. The surface-attachable ATRP initiator ([11-(2-chloro)propionyloxy]undecyl-dimethylchlorosilane, CPU−dMCS), was synthesized by the hydrosilylation of 10-undecen-1-yl 2-chloropropionate with dimethylchlorosilane in the presence of Karsted catalyst (Supporting Information, Figure S25).[32,33] First, the synthesis of 10-undecen-1-yl 2-chloropropionate is described below. Triethylamine (4.88 g, 48.2 mmol), 10-undecen-1-ol (6.81 g, 40.0 mmol), and dry tetrahydrofuran (45 mL) were mixed for 10 min in an ice bath followed by dropwise addition of 2-chloropropionyl chloride (5.08 g, 40.0 mmol) over 5 min. The mixture was stirred at 0° for 2 h and at room temperature for 12 h and then diluted with hexane (100 mL) and washed with 10% HCl aqueous solution, sodium bicarbonate water, and purified water. The organic phase was dried with calcium sulfate. The crude compound was purified by column chromatography with hexane/ethyl acetate mixed solvent (25/1 v/v) as an eluent. After the solvent was removed under reduced pressure, 7.72 g (74%) of 10-undecen-1-yl 2-chloropropionate as a colorless oil was obtained (Supporting Information, Figure S29). Next, 10-undecen-1-yl 2-chloropropionate (0.67 g, 2.57 mmol), dimethylchlorosilane (1.21 g, 12.81 mmol), and Karstedt catalyst (10.0 μL) were added to a dry flask. The mixture was stirred at room temperature for 12 h while the reaction was monitored by ^{1}H NMR. After the excess reagent was removed under reduced pressure, 0.83 g (91%) of the surface-attachable ATRP initiator as a colorless oil was obtained (Supporting Information, Figure S30).

^{1}H NMR (δ [ppm], 270 MHz, $CDCl_3$): 0.401 (6H, s, -Si-CH_3), 0.832 (2H, t, −Si−CH_2−), 1.19−1.48 (16H, m, −CH_2−), 1.57−1.75 (5H, m, −COO−CH_2−CH_2-, CH_3-CHCl-), 4.17 (2H, t, −COO−CH_2−), 4.35 (1H, q, CH_3−C*H*Cl-), 0.030 (6H, s, CH_3−Si−O−Si−), 0.127 (2H, t, −Si−O−Si−CH_2−).

Preparation of [*11-(2-methyl)propionyloxy*]*undecyldimethylchlorosilane* (*MPU−dMCS*) *as an ATRP-Inactive Alkyldimethylsilane Derivative*. A dimethylchlorosilane derivative with a similar chemical structure to CPU−dMCS ([11-(2-methyl)propionyloxy]undecyl-dimethylchlorosilane, MPU−dMCS) was synthesized by hydrosilylating 10-undecen-1-yl 2- methylpropionate with dimethylchlorosilane in the presence of Karsted catalyst (Supporting Information, Figure S26).[32,33] The preparation of 10-undecen-1-yl 2-methylpropionate conforms to that of 10-undecen-1-yl 2-chloropropionate as follows. Triethylamine (4.88 g, 48.2 mmol), 10-undecen-1-ol (6.81 g, 40.0 mmol), and dry tetrahydrofuran (45 mL) were mixed for 10 min in an ice bath followed by the dropwise addition of 2-methylpropionyl chloride (4.26 g, 40.0 mmol) over 5 min. The mixture was stirred at 0° for 2 h and at room temperature for 12 h; then, it was diluted with hexane (100 mL) and washed with 10% HCl aqueous solution, sodium bicarbonate water, and purified water. The organic phase was dried with calcium sulfate. The crude compound was purified by column chromatography with hexane/ethyl acetate mixed solvent (25/1 v/v) as an eluent. After the solvent was removed under reduced pressure, 8.85 g (92%) of 10-undecen-1-yl 2-methylpropionate as a colorless oil was obtained (Supporting Information, Figure S31). The preparation of MPU−dMCS conforms to that of CPU−dMCS as follows. 10-undecen-1-yl 2- methylpropionate (0.62 g, 2.57 mmol), dimethylchlorosilane (1.21 g, 12.81 mmol), and Karstedt catalyst (10.0 μL) were added to a dry flask. The mixture was stirred at room temperature for 12 h while the reaction was monitored by ^{1}H NMR. After the excess reagent was removed under reduced pressure, 0.65 g (76%) of the dimethylchlorosilane as a colorless oil was obtained (Supporting Information, Figure S32).

^{1}H NMR (δ [ppm], 270 MHz, $CDCl_3$): 0.394 (6H, s, -Si-CH_3), 0.810 (2H, t, −Si−CH_2−), 1.15 (6H, d, CH_3−CH−), 1.21−1.48(12H, m, −CH_2−), 1.52−1.69(2H, m, −COO−CH_2−CH_2−), 2.53 (1H, m, CH_3−C*H*−), 4.05 (2H, t, −COO−CH_2−), 0.022 (6H, s, CH_3−Si−O−Si−), 0.119 (2H, t, −Si−O−Si−CH_2−).

Preparation of ATRP Initiator-Deposited Silicon Wafer. A CPU−dMCS and/or MPU−dMCS-functionalized surface was prepared according to the literature[32,33] with small modifications. A silicon wafer was cut into 1.0 × 1.5 cm pieces and placed in a UV/ozone treatment chamber (UV253S, Filgen) filled with pure oxygen to clean the surface for 30 min. The freshly cleaned silicon wafers were placed into anhydrous toluene containing the CPU−dMCS and/or MPU−dMCS (with a total concentration of 5.08 mM). The recipes for CPU−dMCS and/or MPU−dMCS mixed monolayers are shown in Table 1. The silicon wafers were allowed to stand in this solution for 84 h at 60 °C. The resultant samples were isolated, ultrasonically cleaned by dry toluene, rinsed sequentially with toluene and ethanol, and dried in a N_2 stream. The samples were stored at room temperature in a dried, N_2-filled glovebox when not used in the following reactions.

General Procedure for Synthesis of Grafted PNIPA from ATRP Initiator-Modified Silicon Wafers. The best approach to the synthesis of a well-defined high-density brush is the "grafting from method" using a surface bound initiator.[34−36] The surface initiated ATRP of NIPA onto a silicon wafer and Au-deposited mica has been reported, but in many cases, the authors do not give molecular weight and polydispersity data.[37−48] Judging by our additional examinations, many cases of surface-initiated ATRP of NIPA on a flattened surface such as silicon, the thickness of the grafted PNIPA membranes cannot be well-controlled according to

Table 1. Synthesis of CPU−dMCS and/or MPU−dMCS Mixed Monolayers

sample no.	CPU−dMCS (μL)	MPU−dMCS (nL)	CPU−dMCS: MPU−dMCS (mol/mol)
1	60.0 (5.08 mmol)	0 (0 mmol)	100:0
2	45.0 (3.81 mmol)	17.7 (1.27 mmol)	75:25
3	30.0 (2.54 mmol)	35.4 (2.54 mmol)	50:50
4	15.0 (1.27 mmol)	53.2 (3.81 mmol)	25:75
5	6.0 (0.51 mmol)	63.8 (4.57 mmol)	10:90
6	0 (0 mmol)	67.3 (5.08 mmol)	0:100

Table 2. Synthesis of PNIPA Brush by Surface-Initiated ATRP in Various Reaction Times

sample no.	[M]:[I]:[Cu_I]:[L] (M/DMSO) (w/w)	reaction time (h)	conversion(%)	$M_{n\text{-theol}}$/ 10000	$M_{n\text{-GPC}}$/ 10000	M_w/M_n	film thickness at dry state (nm)	graft density (chains/ nm^2)
1′		0.25	25	2.8	3.1	1.34	23	0.48
2′		1	49	5.5	5.1	1.25	41	0.52
3′	1000: 1:1:1 (1/2)	2	64	7.2	6.0	1.25	49	0.52
4′		5	76	8.6	7.3	1.19	58	0.52
5′		10	81	9.2	8.5	1.21	62	0.47

the living polymerization system (Supporting Information, Figures S11 and S14b). Moreover, the densities of the grafted PNIPA membranes are in diluted or semidiluted regions, and as a result, the intermolecular interaction between grafted polymers is not significant due to the poor choice of the polymerization systems. However, ATRP is attractive because it can provide good control over predictable polymer molecular weight, PDI and end groups as long as the conditions are suitable.

The appropriate selection of experimental conditions, such as initiators, catalysts, solvents, and temperatures for ATRP, results in polymers with high conversions, low PDIs, and defined average polymer molecular weights. So far, ATRPs of acrylamide derivatives have been attempted with several conditions, but these attempts were fraught with difficulty in many cases.[49,50] Catalyst inactivation, low values of ATRP equilibrium constants, and displacement of the terminal halide have been recognized as complicating factors during polymerization. However, recent research has included solution approaches for ATRP of acrylamide derivatives.[51,52] Some researchers believe that Cu salts tend toward the polymer chain ends and stabilize the radicals. This stabilization retards the deactivation step in ATRP and produces an unacceptably high concentration of radicals that leads to spontaneous termination reactions. These results were attributed to the occurrence of slow deactivation in conjunction with fast activation and to the loss of bromine end groups through a cyclization reaction involving nucleophilic Br displacement by the penultimate amide nitrogen. The use of Cl instead of Br should decrease the risk of nucleophilic substitution of the halogen from the dormant chain end. When linear amines or bipyridine-based ligands were employed, acrylamide derivatives were not polymerized controllably by ATRP. The combination of a chloropropionate functionalized initiator and Me_6TREN as the ligand was found to be an effective system for the ATRP of acrylamide derivatives.[51−53] Consequently, using alkyl chlorides rather than bromides as initiators in conjunction with Me_6TREN as a ligand improved control. Moreover, DMSO was chosen as the solvent for ATRP of NIPA on the premise that a solvent with the electron-pair donating property could interact with the amide groups of NIPA and thus reduce their interaction with both the catalyst and the propagating chain end. In addition, DMSO is a good solvent for PNIPA over a very wide range of temperatures. The success of the ATRP of NIPA in pure water has been reported recently, but we did not choose the water reaction system because of the high sensitivity of the PNIPA configuration in an aqueous solution.[54] Thus, we used CPU−dMCS as a surface-modified initiator, CuCl/Me_6TREN as a catalytic system, and DMSO as a solvent.

To form a PNIPA brush from the surface bound initiator, ECP was added as a free initiator in the reaction solution to control the polymerization process. Without the free initiator, the concentration of Cu^{II} complex produced from the reaction at the surface becomes too low to deactivate the active chain ends of polymers with a sufficiently high rate. The concentration of Cu^{II} complex can be raised and automatically adjusted by adding the free initiator.[24] Furthermore, we can obtain information about the polymerization product, such as the average polymer molecular weight and PDI in the brush, by observing those of the free polymer because good agreement in the number-average molecular weight (M_n) and PDI between the graft and free polymers has been confirmed by several research groups.

In a typical experiment ([NIPA]:[ECP]:[CuCl]:[Me_6TREN] = 1000:1:1:1), a 10 mL stoppered test tube was loaded with NIPA (3.39 g, 30 mmol) and 3.40 g of DMSO as the solvent (Supporting Information, Figure S27). The solution was sealed with a three-way stopcock and cycled three times between argon gas and a vacuum to remove the oxygen. ECP (4.1 mg, 0.03 mmol) as a free initiator, CuCl (3.0 mg, 0.03 mmol) with Me_6TREN (6.9 mg, 0.03 mmol) as a catalyst, and the initiator-modified silicon wafer were then added to the solution in a glovebox. The sealed test tube was placed into a water bath with a temperature of 20 °C, and polymerization occurred. (Tables 2, 3, and 4 show all the polymerization recipes.) A small amount of hydroquinone was added to the test tube to stop the polymerization after a predetermined time. The newly formed polymer grafted membrane was washed with ethanol with sonication for 1 min and rinsed with the EDTA solution, distilled water, ethanol to remove unreacted species, the catalyst, and free polymers and dried under a N_2 stream. The resultant polymer solution was used to determine the monomer conversion by ^{1}H NMR in DMSO-*d* and to examine the average polymer molecular weight and polydispersity index (PDI) by gel permeation chromatography (GPC).

Characterization. *XPS Analysis of Monolayer*. Chemically grafted monolayers were characterized by X-ray photoelectron spectroscopy (XPS) using an ESCA-3300 (Shimadzu) with an Mg Kα X-ray at 10 mA and 30 kV over 16 scans. All binding energies were referenced to Si 2p at 99.5 eV.

AFM Analysis of Monolayer and Polymer Brush. The thicknesses of the dried membranes were measured by Nanopics 2100 (SII NanoTechnology) with a NPX1CTP003 cantilever (SII NanoTechnology). Surface images of the CPU−dMCS and/or MPU−dMCS-functionalized silicon wafers and the polymer grafted membranes grown on the silicon wafers were obtained using an SPA400/SPI3800N system (Seiko Instrument) with a silicon cantilever (SI-DF20) in AFM mode. The thicknesses and the roughness of the swollen polymer grafted membranes were also measured by the same apparatus at different temperatures.

Equilibrium Contact Angle Measurements. Contact angle measurements were made with FACE CA-XP (Kyowa Interface Science) using a sessile water droplet in air and captive air bubble within a water-filled temperature controlled cell by a circulating water bath (LAUDA E-200) (Supporting Information, Figure S21). A static contact angle, θ, of a water droplet

Table 3. Synthesis of PNIPA Brush by Surface-Initiated ATRP at Various Ratios of Monomer and Free Initiator

sample no.	[M]:[I]:[Cu_I]:[L] (M/DMSO) (w/w)	reaction time (h)	conversion (%)	$M_{n\text{-theol}}$/ 10000	$M_{n\text{-GPC}}$/ 10000	M_w/ M_n	film thickness at dry state (nm)	graft density (chains/nm^2)
6′	100:1:1:1 (1/2)	7	97	1.1	1.3	1.16	9	0.47
7′	300:1:1:1 (1/2)	7	90	3.1	3.3	1.19	26	0.51
8′	400:1:1:1 (1/2)	8	90	4.1	4.1	1.17	33	0.52
9′	1000:1:1:1 (1/2)	10	81	9.2	8.5	1.21	62	0.47
10′	2000:1:1:1 (1/2)	18	82	18.6	16.2	1.29	121	0.48
11′	3000:1:1:1 (1/2)	24	82	27.8	27.3	1.35	223	0.53

Table 4. Synthesis of PNIPA Brush by Surface-Initiated ATRP at Various Ratios of Monomer and Free Initiator and Various Initiator Densities

sample no.	[M]:[I]:[Cu]:[L] (M/DMSO) (w/w)	initiator density[a] (%)	conversion (%)	$M_{n\text{-GPC}}$/10000	M_w/ M_n	film thickness at dry state (nm)	graft density (chains/nm^2]
12′	400:1:1:1 (1/2)	100	90	4.1	1.17	33	0.52
13′	400:1:1:1 (1/2)	50	89	4.1	1.17	16	0.24
14′	400:1:1:1 (1/2)	10	92	3.8	1.15	4	0.06
15′	1000:1:1:1 (1/2)	100	81	8.5	1.21	62	0.47
16′	1000:1:1:1 (1/2)	75	86	11.1	1.21	49	0.29
17′	1000:1:1:1 (1/2)	50	79	10.2	1.21	44	0.28
18′	1000:1:1:1 (1/2)	25	83	11.2	1.18	23	0.14
19′	1000:1:1:1 (1/2)	10	88	10.7	1.24	8	0.05
20′	2000:1:1:1 (1/2)	100	82	16.2	1.30	121	0.48
21′	2000:1:1:1 (1/2)	50	84	16.8	1.31	66	0.25
22′	2000:1:1:1 (1/2)	10	85	16.7	1.28	11	0.04
23′	2000:1:2:2 (1/2)	100	88	18.7	1.40	140	0.48
24′	2000:1:2:2 (1/2)	10	90	18.7	1.41	17	0.06

[a] As the contact angle of water on the monolayers of CPU−dMCS/MPU−dMCS monotonically decrease with the amount of CPU−dMCS in the precursor solutions, the initiator density (mol % of CPU−dMCS of total amount of CPU−dMCS and MPU−dMCS) in the monolayer is the same value of that in the precursor solutions.

(ca. 1 μL) on the surfaces of the CPU−dMCS- and/or MPU−dMCS-functionalized silicon wafers was determined 5 times to obtain a reliable average value by the sessile drop method at 20 °C. In the captive air bubble method, the polymer grafted membranes were immersed face-down in Millipore water to attain an equilibrium swollen state in the temperature controlled cell for 30 min before bringing the air bubble into contact with the surfaces of the membranes. As a result, an air bubble (ca. 3 μL) was trapped underneath the polymer grafted membranes in water and equilibrated until the chemical potential of water vapor in the vapor-saturated air bubble equaled that of liquid water.[55] Achieving an equilibrated contact angle of the air bubble took more than 30 min depending on the water temperature. Then, the equilibrated contact angle of the air bubble was recorded after waiting an adequate amount of time. The reported values are averages of five measurements from different areas of the sample surface.

Gel Permeation Chromatography (*GPC*). Average polymer molecular weights and PDIs were determined by the GPC system. A GPC measurement was performed using GL-7410 HPLC (GL Science), KD-804 and KD-805 columns (Shodex) and a GL-7454 refractive index detector (GL Science) maintained at 20 °C. For PNIPA analysis, narrow-disperse polymethacrylate standards were used for calibration. The eluent was a DMF:chloroform 50:50 (v/v) mixed solvent including 5 mM of LiCl at a flow rate of 1.0 mL min^{-1}. The samples for analysis were prepared by directly diluting a given amount of the reaction mixture in the eluent for GPC to obtain a polymer concentration of about 1 wt %.

^{1}H NMR Spectroscopy. Conversions for polymerizations were estimated by ^{1}H NMR spectroscopy. ^{1}H NMR spectra were measured on JNM-GSX270 or JNM-A400 spectrometers with samples dissolved in DMSO-*d*. The direct analysis of the polymer from the unpurified reaction mixture should give more representative values of the polydispersities and the conversions. Thus, the reaction mixtures were diluted by DMSO-*d* to obtain solute concentrations of about 1 wt % and used for ^{1}H NMR analysis. The conversion of monomers to polymer was calculated by comparing the peak areas of monomer signals at 5.5 ppm (1H, vinyl proton of NIPA monomer) with the polymer signal at 3.8 ppm (1H, lone proton of the *N*-isopropyl group of both NIPA monomer and PNIPA), corrected for the contribution of monomers (Supporting Information, Figure S28).

Fourier Transform Infrared Spectroscopy (*FT-IR*). Transmission IR spectra of the polymer grafted membranes on the silicon substrates were measured using an FTS 6000 FT-IR spectrometer with a HgCdTe semiconductor (MCT) detector (Bio-Rad Laboratories). For dried polymer grafted membranes on the silicon substrates, the samples were placed in the chamber of the spectrometer in a nitrogen atmosphere. A surface cleaned bare silicon wafer was used as a blank sample to obtain differential spectra (Supporting Information, Figures S34 and S35). For the water swollen polymer grafted membrane on the silicon substrate, the dried sample was placed between two CaF_2 rectangular plates (22 × 41 mm, thickness 4 mm) with a 6-μm thick Mylar film (Supporting Information, Figure S38). After D_2O was injected into the cell, the cell was attached to a metal cell holder and a temperature controlled jacket with a circulating water bath (LAUDA E-200) and placed in the chamber of the spectrometer under a nitrogen atmosphere. An electronic thermometer (AS ONE TM-300) with a precision of ±0.1 °C continuously monitored the temperature of the cell. A total of 128 scans were accumulated for each spectrum at a 4 cm^{-1} spectral resolution at a given temperature. Data analyses of the IR spectra, such as curve fitting, baseline subtraction, and waveform separation, were performed with Origin 6.0 (Origin Lab), Resolutions Pro (Varian) and SPNIA, which was supplied by Prof. Katsumoto.

Results and Discussion

When fabricating a high-density brush composed of PNIPA, it is important to choose the appropriate surface conditions for attaching PNIPA to one end and the preparatory procedure to obtain a high-density brush. In this study, we used a silicon wafer as an underlying substrate because of its flatness, smoothness, and the ease with which its surface chemicals can be modified. Because the ATRP method was applied to obtain PNIPA in a well-controlled polymerization method, the surface of the silicon wafer was initially modified by an ATRP initiator with various surface densities. Then, low-dispersity PNIPA chains were grown by ATRP in a variety of reaction conditions from the surface

bound initiator. Here, we explain each step used to make the high-density brush composed of PNIPA and present several of its physicochemical properties.

Preparation of Silicon Surface Modified with ATRP Initiator. A number of different chemical structures of surface silanized membranes composed of organosilanes on a silicon wafer, especially for di- and trihydrolyzable organosilanes, can be produced depending on the reaction conditions because these organosilanes can react not only with Si−OH groups on the surface oxide layer of a silicon wafer but also with each other in the silanized membranes obtained.[56] Monohydrolyzable organosilanes are attractive in terms of the reproducibility of surface structures of silanized membranes on a silicon wafer.[56,57] However, because the reactions of the alkyldimethylsilane derivatives with only one hydrolyzable group at the solution-solid interface are very slow in the later stages of the reaction, long reaction times are necessary to achieve maximum bonding density. On the basis of our previous results, the reaction continues over days and is not complete within 1 or 2 days (Supporting Information, Figures S4 and S6). Some reports using carefully optimized conditions showed that densely packed monolayers with alkyldimethylsilane derivatives were highly hydrophobic, with water contact angles of about 110°.[56,57] In contrast, however, the value of the contact angle of the water drop for our monolayer composed of MPU−dMCS reached about 87°. This difference is not due to kinetic limitations but is inherent to the pretreatment of a silicon wafer surface and the reaction conditions with the alkyldimethylsilane derivatives. A bare silicon surface is usually covered by a native oxide layer with a thickness of 2−10 Å.[58] To obtain a surface of the oxide layer saturated with OH groups, the standard RCA treatment developed by the Radio Corporation of America should be used. Meanwhile, UV/ozone cleaning eliminates organic contaminants but does not affect the oxide layer; thus, the surface of the oxide layer that we used in this study was not fully saturated with OH groups.[59] Moreover, because the presence of a base for the surface modification of organosilanes is required to achieve a high surface density, our systems probably did not reach densely packed states.[56] Even so, our resultant monolayers meet the requirement to fabricate the high-density polymer brushes due to the larger steric hindrance of polymer chains.

The surface density of silanols on hydroxylated silica covering the surface of a silicon wafer is 4.6 Si−OH groups/nm^2, and approximately 60% of the groups can react with alkyldimethylsilanes with one hydrolyzable group.[56,60,61] As a result, the cross-sectional area of the alkyldimethylsilyl groups in the densely packed monolayer was 32−38 Å^2, which is a lower density than that of self-assembled alkyltri-hydrolyzable-silane-derived monolayers on a silicon wafer (∼20 Å^2).[57] At the same time, because the cross sectional area of typical acrylate polymers that have a substantially stretched form in the brush state at the solid surface is ∼200 Å^2,[62] i.e., only 1 of 5 or 6 alkyldimethylsilane derivatives, which act as ATRP initiators bound to the surface, is expected to initiate polymerization for the densely packed monolayers. Thus, we do not need to use densely packed monolayers composed of ATRP initiative alkyldimethylsilane derivatives to generate densely packed, i.e., high-density, polymer brushes.

The successful deposition of CPU−dMCS that acts as an ATRP initiator was verified by XPS. Parts a−c of Figure 1 show XPS data of (a) C 1s, (b) Cl 2s, and (c) Cl 2p, respectively, for the CPU−dMCS monolayer prepared by immersion into the CPU−dMCS toluene solution for 84 h at 60 °C. The asymmetric C 1s peak is composed of three components as follows: (1) a small peak around 288.5 eV corresponding to unsaturated

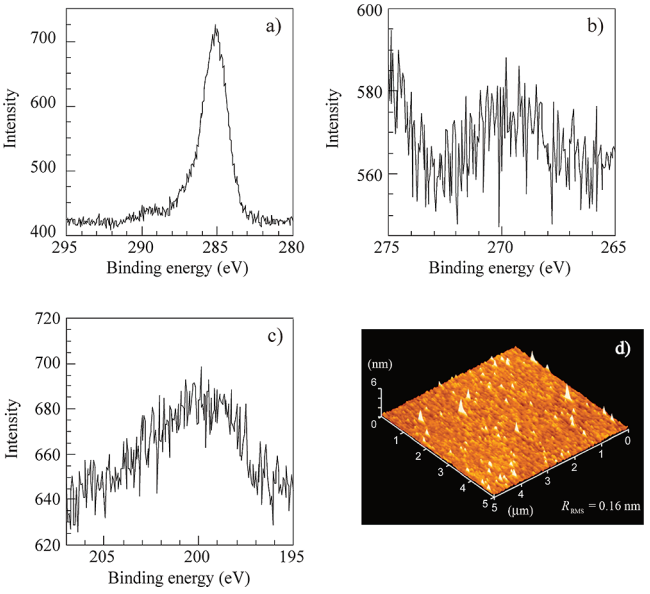

Figure 1. XPS data of (a) C 1s, (b) Cl 2s, and (c) Cl 2p for CPU−dMCS modified silicon wafer. (d) AFM image of CPU−dMCS modified silicon wafer.

carbon in the carbonyl group, (2) a band around 285.6 eV due to a carbon adjoining the carbonyl group and carbon in the −OCH_2 group, and (3) a band at around 284.7 eV attributed to saturated carbon in the alkyl chain,[63] which proves the immobilization of CPU−dMCS on a silicon wafer (Figure 1a). Initiator immobilization is also apparent from the appearance of chlorine peaks in the XPS data (Figure 1b,c).

Figure 1d shows an AFM image of the monolayer composed of CPU−dMCS. There are no microstructural defects, such as holes and aggregates in the monolayer. The value of the root-mean-square roughness (R_{rms}) is 0.16 nm over 25 μm^2, which demonstrates that the surface is very smooth. We used CPU−dMCS and MPU−dMCS, which has no reactive site, with vinyl monomers to make mixed monolayers to control the polymer density. CPU−dMCS and MPU−dMCS are both alkyldimethylsilane derivatives with a long alkyl chain and one hydrolyzable group. Since these derivatives are similar in chemical structure, homogeneously mixed membranes must be formed on the surface of a silicon wafer depending on the composition in the precursor solutions. We formed mixed monolayers on a silicon wafer using stock solutions ranging from 0% to 100% of CPU−dMCS. Figure 2a shows the change in the water contact angle for the mixed monolayers prepared by immersion into the various CPU−dMCS/MPU−dMCS mixed toluene solutions for 84 h at 60 °C. The water contact angles on the monolayers monotonically decreased with the amount of CPU−dMCS in the precursor solutions. The increase in the composition of CPU−dMCS in the monolayers on a silicon wafer was confirmed by the decrease in the contact angle because CPU−dMCS has a slightly more hydrophilic character than MPU−dMCS. The contact angle measurement implies that the ratios of CPU−dMCS and MPU−dMCS in the monolayers are at least similar to the ratios in the stock solutions.

The Cassie equation is an empirical expression that relates the macroscopic contact angle of a pure fluid on an atomically smooth, but chemically heterogeneous, solid surface,

$$\cos\theta = f_1 \cos\theta_1 + f_2 \cos_2 \qquad (1)$$

where f_i is the area fraction of component i and θ_i is the contact angle of the fluid on a surface of pure i.[64] When the

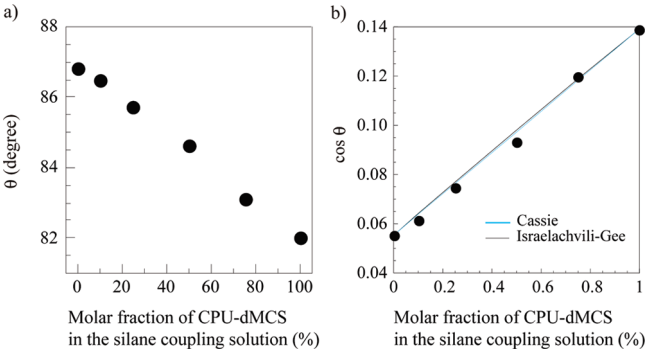

Figure 2. (a) Static contact angle of water on CPU−dMCS/MPU−dMCS modified silicon wafer at 20 °C as a function of molar fraction of CPU−dMCS in silane coupling reaction solution. (b) Experimental result in part a compared with two theoretical treatments, the Cassie equation and the Israelachvili−Gee equation.

size of the domains, composed of each component, approaches molecular dimensions, the Israelachvili−Gee equation should be used.[65]

$$(1+\cos\theta)^2 = f_1(1+\cos\theta_1)^2 + f_2(1+\cos\theta_2)^2 \qquad (2)$$

In Figure 2b, the simulation results using both the Cassie equation and the Israelachvili-Gee equation for the water contact angles are compared with the experimental data. Because there is no difference between the two simulation results due to the small change in θ_1 and θ_2, good agreement is seen between each simulation result and the experimental results. Thus, we can apply either equation to analyze a chemically heterogeneous system with a small change between the contact angles of the fluid on each surface of pure *i*. This conclusion must be applicable to any contact angle measurement method, such as the captive bubble method.

ATRP of NIPA for Preparation of Grafted Membrane. The results for the ATRP of NIPA under the same reaction conditions, except for the reaction time, are summarized in Table 2 and Figure 3. The ATRP in this condition provides high conversion, reaching about 81% in 10 h, but the first-order kinetic plot shows noticeable curvature (Figure 3a). However, the GPC traces were reasonably symmetrical with no shoulders and tailing even at higher conversions (Figure 3b). Moreover, M_n increased linearly with conversion, and the PDI remained low throughout the polymerization (Figure 3c), which indicates that the growing centers were not lost during the reaction. Thus, the apparent curvature of the plot in Figure 3a is attributed to a progressive reduction of the concentration of the available catalyst rather than chain termination. M_n obtained by GPC was comparable to the target molecular weight at each time point, which also demonstrates that the initiator is efficient. Additionally, the PDI decreased from 1.34 to 1.21 with increasing conversion, which also proves the living process.[23]

The thicknesses of the dried polymer grafted membranes (L_d) on the silicon wafers were determined by AFM imaging across the boundary of a scratched and an unscratched region. An almost linear relationship between the brush thickness and the molecular weight can be seen in Figure 3d (Supporting Information; Figure S34 contains the IR spectra). These data demonstrate that chain growth from the surface of the substrate is also a controlled process in keeping with the nature of this ATRP reaction in solution. In this condition, L_d can be grown to over 60 nm. The value of R_{rms} for sample no. 5′, which is the thickest membrane in this series, is 0.60 nm over 25 μm^2 using the AFM (Figure 3e), which shows that the surface is very smooth (Supporting Information; Figure S33 has an optical image). To obtain a thicker dried grafted membrane with the same graft density, we tried to raise the ratio of NIPA to initiator because the theoretical M_n for an ideal ATRP reaction can be increased by increasing the ratio. Table 3 and Figure 4 show the results for the ATRP of NIPA depending on the ratio of NIPA to initiator. The experimentally obtained M_n is also very consistent with the theoretical value of M_n, and the PDI remains narrow even at higher molecular weights (Figure 4a). A linear increase in the thickness up to over 200 nm with a chain length was observed (Figure 4b), which indicates that the chain growth from the surface is a controlled process with a degree of living character to it and that the thickness of the membrane, which corresponds to the chain length, can be easily manipulated. As above, we have shown that the ATRP of NIPA using the combination of ECP as an initiator and CuCl/Me_6TREN as a catalytic system in DMSO at 20 °C was successful in producing narrow disperse PNIPA with high conversion and good molecular weight control.

From the slope of the line in Figure 3d and 4b, the graft density σ can be estimated by the following equation[66]

$$\sigma = L_d \rho N_A / M_n \qquad (3)$$

where ρ is the mass density of PNIPA (1.042 g/cm^3) (Supporting Information, Figure S36) and N_A is Avogadro's number. The values of L_d and σ for the samples are listed in Table 2 and Table 3, respectively. The graft densities are virtually constant around 0.5 chain/nm^2: the cross sectional area of the grafted PNIPA is ~200 Å^2. For comparison, we calculated the contour lengths of the directionally fully stretched PNIPA chains (L_c) using a C−C bond length of 1.54 Å and a ∠CCC of 110.5° based on M_w and show the result with the experimentally obtained values of L_d (Figure 5).[67] For any samples, the thickness in the dry state is more than 25% of the fully stretched polymer chain length (L_d/L_c), which indicates that the polymers are directionally extended perpendicular to the surface of the substrate compared with their unperturbed dimensions.[34,35] This result shows that PNIPA chains in these dried membranes are directionally extended states with an extremely high graft density regardless of the molecular weight.

When we used the CPU−dMCS/MPU−dMCS mixed monolayer on the silicon wafers shown above, the graft density of PNIPA is also controlled by the initiator density (Figures 6 and S35 for IR spectra). If the alkyldimethylsilane derivatives formed densely packed states, the graft density of PNIPA could be constant above ca. 20% of the initiator density. However, the graft density of PNIPA is proportional to the initiator density, which also suggests that the alkyldimethylsilane derivative modified substrates did not reach the densely packed state. As above, we successfully demonstrated that the ATRP of NIPA at the initiator modified silicon surfaces could be conducted in a well-controlled manner, which resulted in PNIPA grafted membranes with tunable polymer thickness and density.

Change in Thickness of High-Density Grafted Membrane of PNIPA in Water with Changing Temperature. Figure 7 shows the change in the thickness of the high-density grafted membrane of PNIPA with L_d of 121 nm (sample no. 10′) in water with changing temperature. Polymer chains grafted on a flat substrate at one end with an extremely high graft density can be stretched further in good solvents. The greatest value of L_s/L_c of 0.47, where L_s is the thickness of the grafted membrane in a solvent, indicates that the graft chains in this membrane in water at 19 °C are in a highly extended state: PNIPA chains in the membranes under this condition form so-called "high density brushes". Even at the fully collapsed state in water at 36 °C, the value of L_s/L_c is 0.32, which indicates that the polymer chains are in a more extended state than the dried state. This observation suggests

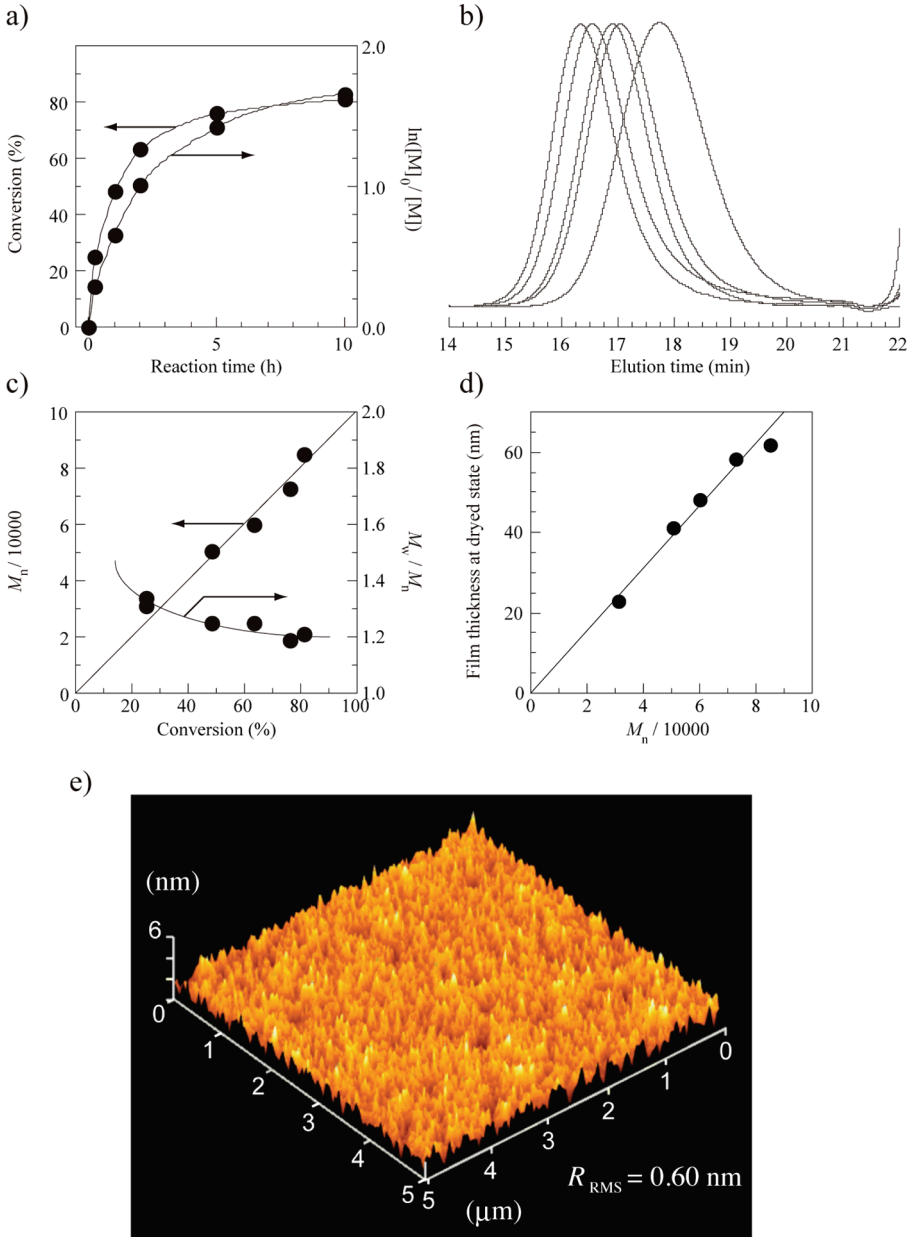

Figure 3. (a) Monomer conversion and kinetic plot with polymerization time during ATRP of NIPA. (b) Evolution of GPC traces with polymerization time during ATRP of NIPA. (c) Number-average molecular weight, M_n, and polydispersity index (M_w/M_n) versus conversion plots. The straight line corresponds to the theoretical M_n versus conversion. (d) Plots of dried thickness of polymer grafted membrane versus M_n. (e) AFM image of densely grafted dried PNIPA membrane, sample no. 5′.

that the interaction between the PNIPA chains and water molecules in the membrane is significant even in the fully collapsed state. In addition, the gradual collapse of the PNIPA-grafted membrane was assessed by measuring its thickness by AFM in water with increasing temperature. Theoretical predictions suggested that the collapse of surface-tethered polymer brushes accompanying the solubility transition proceed continuously over a much broader range as the solvent quality decreases, which is distinct from the behavior of free flexible chains adopting random coil conformations in solution.[68] The change in the thickness of our high-density brush in water is amenable to the theory.

FT-IR to Observe Molecular Behavior of PNIPA in Grafted Membrane under Water. To observe the molecular behavior of the polymer chains in the membranes, we measured the FT-IR spectra of the grafted membranes in water at several temperatures. FT-IR observation is a powerful method to elucidate interaction information at the molecular level. In our intended system, the vibrations of amide groups in PNIPA chains are highly sensitive to changes in the conformation of the polymer chains and in the interaction with solvent molecules.[69] In this study, we used D_2O as a solvent instead of H_2O because the bending vibration band of H_2O observed around 1600 cm^{-1} overlaps the amide I band, whereas that of D_2O appears around 1200 cm^{-1}. During the change in temperature across the LCST for the PNIPA linear polymer in a solution state, an isosbetic point can be observed at 1637 cm^{-1} (Supporting Information, Figure S39). Isosbetic behavior means that there exist two absorption peaks that have a constant position, and only the intensities of these peaks change (Supporting Information, Figure S40). There are various views on the assignment of these peaks.[69−72] Maeda et al. state that the lower wavenumber peak observed around 1625 cm^{-1} may be assigned to the C═O group that is bound to water molecules, and the higher one observed

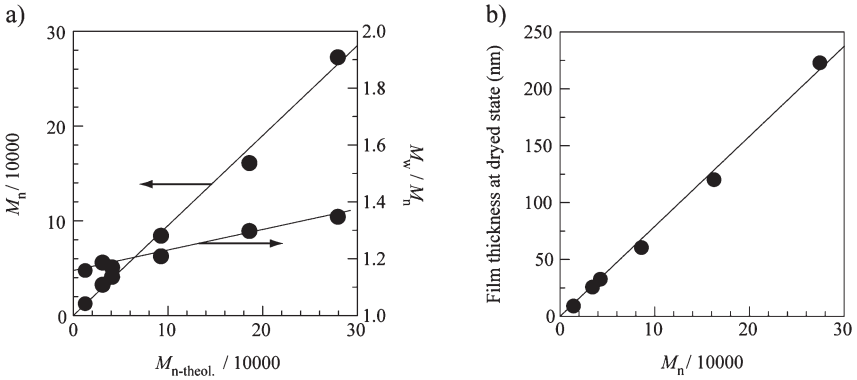

Figure 4. (a) Number-average molecular weight, M_n, and polydispersity index (M_w/M_n) versus theoretical M_n plots. (b) Plots of dried thickness of polymer grafted membrane versus M_n.

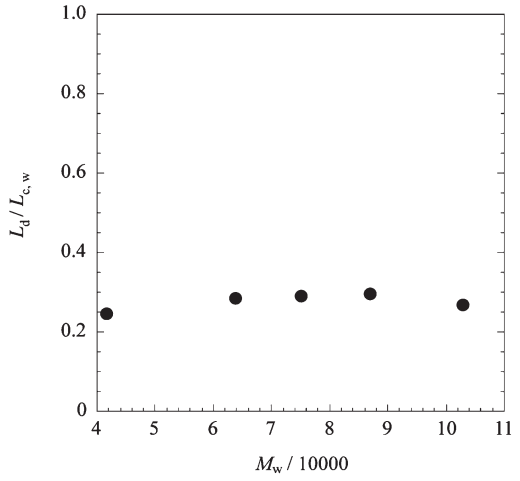

Figure 5. Plots of $L_d/L_{c,w}$ versus weight-average molecular weight, M_w.

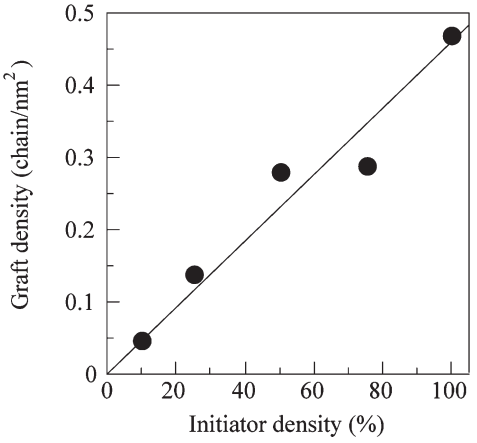

Figure 6. Graft density of PNIPA versus initiator density estimated from the ratio of CPU−dMCS and MPU−dMCS in the stock solutions.

around 1650 cm^{-1} may be the C═O group interacting with the neighboring N−H group via hydrogen bonding.[69] On the other hand, Katsumoto et al. propose that the peak at around 1625 cm^{-1} is mainly due to a stretching vibration of the C═O group forming a strong hydrogen bond with the neighboring N−H group, while the peak at around 1650 cm^{-1} may be due to the free C═O group.[70] Maeda et al. suppose that PNIPA chains form hydrogen bonding between the amide groups above the LCST, whereas Katsumoto et al. suggest that the hydrogen bonding between the amide groups formed below the LCST is broken above the LCST. Other groups' results using ^{1}H NMR

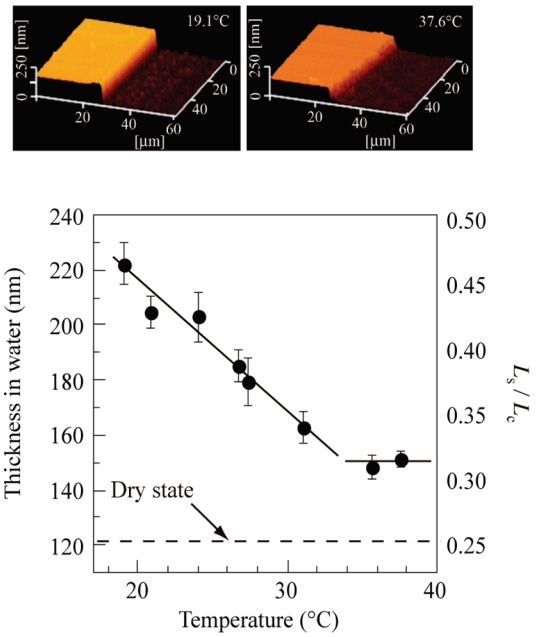

Figure 7. Thickness of high density grafted membrane of PNIPA (sample No.10′) as a function of temperature in water. Pictures show AFM images across the boundary of scratched and unscratched regions in water at different temperatures.

and UV resonance Raman spectra show that the C═O group forms hydrogen bonds with two water molecules lower than the LCST, while the C═O group interacts with only one water molecule on average above the LCST.[71] As described above, there is still room for this argument, but their common view shows that the interaction between the C═O group of the polymer chains and water molecules can be changed drastically in the vicinity of the LCST. Therefore, to investigate the molecular situation of the PNIPA chains in the grafted membranes, we observed the change in the absorption peaks around the vibrations of amide groups in PNIPA resulting from temperature change. Figure 8a shows the amide I band of a high-density polymer brush with a graft density of 0.48 chains/nm^2 composed of PNIPA with an M_n of 187 000 and M_w/M_n of 1.40 measured in D_2O as a result of temperature changes. As the temperature increased from 15.2 to 42.5 °C, the amide I band of PNIPA showed a change in waveform. The amide I band could be separated into two components centered at 1625 cm^{-1} and 1650 cm^{-1} at any temperature. The intensity of the peak at 1625 cm^{-1} decreased with temperature, while that at 1650 cm^{-1} increased. On the other hand, the amide I band of a grafted PNIPA membrane with a graft density of 0.06 chains/nm^2 and

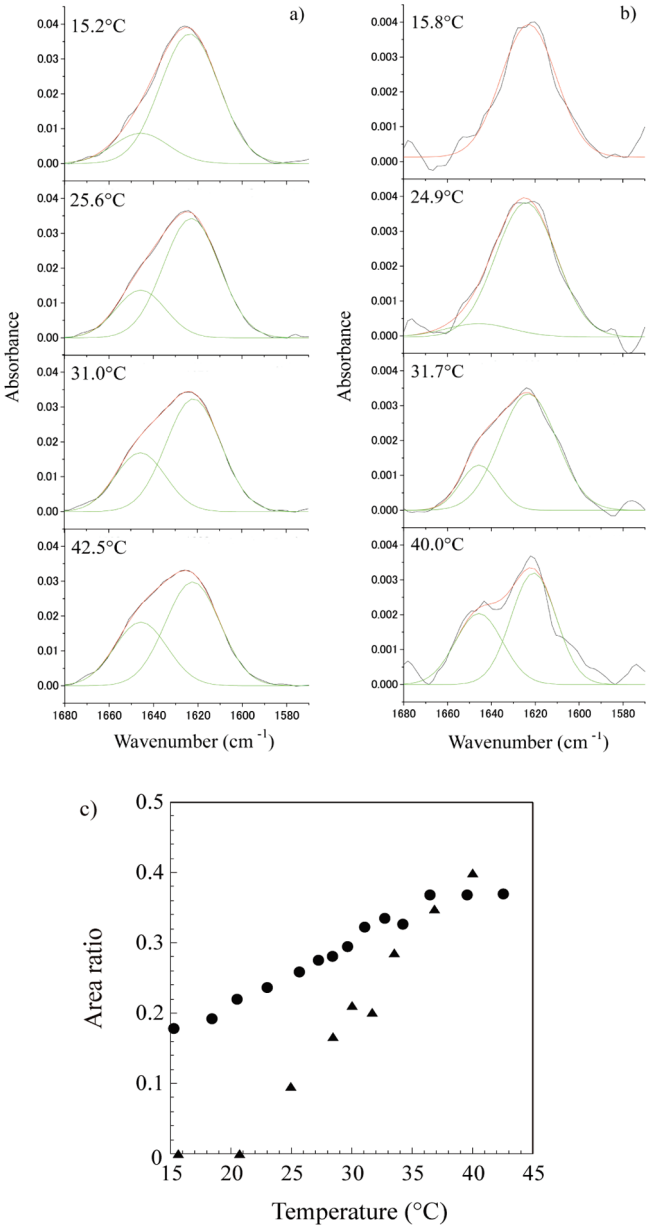

Figure 8. IR absorption spectra in amide I region for PNIPA grafted membranes with different graft densities at several temperatures. Black line: baseline subtracted amide I band, red line: curve fitted peak, green line: best fitted single Gaussian component. (a) $\sigma = 0.48$ chains/nm^2; (b) $\sigma = 0.06$ chains/nm^2. (c) Area ratio for the two components in amide I band versus temperature. The area ratio is calculated as follows: the area ratio = area of 1650 cm^{-1} component/total area of amide I band.

composed of PNIPA with M_n of 187000 and M_w/M_n of 1.41 measured in D_2O at 15.8 °C consists of a single Gaussian component centered at 1625 cm^{-1} (Figure 8b). The second component centered at 1650 cm^{-1} appeared as the temperature increased. This behavior is nearly identical to that of the amide I band of linear PNIPA in a solution state (Supporting Information, Figure S40). Figure 8c shows the temperature-dependent area ratio of these components for each sample. For the lower-density PNIPA grafted membrane, the peak at 1650 cm^{-1}, which does not appear when the solution temperature is below 20 °C, intensifies abruptly as the temperature increases. This increase suggests that the PNIPA chains exhibit a coil−globule-like transition similar to the transition shown by linear PNIPA in a solution (Supporting Information, Figure S41). At the same time, for the densely grafted PNIPA chains on the silicon substrate, the peak at 1650 cm^{-1} accounted for about 18% of the total area of the spectrum shown in Figure 8a at 15.2 °C, which means that the PNIPA chains partly behave like a collapsed state at a sufficiently low temperature. As above, the PNIPA chains in the high-density brush are in a physically constrained state and cannot fully interact with water molecules. As a result, perhaps, the thickness of the membrane changed continuously over a much broader range with changes in temperature.

Contact Angle of Air Bubble underneath PNIPA Grafted Membranes under Water. Through FT-IR observation, we can understand changes in the molecular behaviors of PNIPA on the inside of the grafted membranes, while the molecular behaviors on the surface can be examined by contact angle measurements. The surface thermo-sensitivities of the PNIPA grafted membranes were assessed by the captive air bubble method. Generally, the hydrophilicity/hydrophobicity of material surfaces can be determined by the sessile drop method. To examine the hydrophilicity of water-soluble polymer grafted membranes and hydrogels, however, applying the sessile drop method is inappropriate because of the continuous change in the conformation and swollen state of polymers due to the strong interaction between the polymers and water molecules in addition to the evaporation of water. In contrast, the contact angle measurement using a captive air bubble is a versatile and reproducible technique to quantify the extent of hydrophilicity/hydrophobicity of water-attracting polymeric substrates in contact with water. Figure 9a shows equilibrium contact angles of an air bubble resulting from temperature changes underneath the PNIPA grafted membranes composed of different molecular weights but with the same graft density of approximately 0.5 chains/nm^2 in water. These changes in the contact angles of air bubbles disagree with the past results for polymer grafted membranes composed of PNIPA.[73] For example, at 11 °C when the brush is swollen with water, the contact angle of the air bubble underneath the membrane composed of PNIPA with 85 000 in M_n is about 140°. The contact angle decreased with an increase in temperature up to 24 °C as shown in previous systems, but then jumped up to 142° around 30 °C. Although the net change of the contact angle is small, this temperature-dependent contact angle behavior has not been observed before. The PNIPA brushes, composed of different molecular weights but with nearly identical σ values of around 0.5 chains/nm^2, undergo a similar change, while the absolute values over all temperatures decrease as the molecular weight decreases. The reason for the decrease in θ with the molecular weight is not yet understood, but a similar change is also observed in other thermo-sensitive polymer brushes. The increase in the lateral expansion of the grafted polymers in response to an increased of the thickness may affect the contact angle.[74,75] Compared to roughly prepared PNIPA brushes (Supporting Information, Figures S22 and S23), the contact angles for these precisely prepared high-density PNIPA brushes drop dramatically at lower temperatures while the ones at higher temperatures are almost same or increase only slightly (Figure 9b). Figure 9c shows the equilibrium contact angles of the air bubble underneath the PNIPA grafted membranes with almost the same molecular weights but different graft densities in water with changing temperature. With the decrease in graft densities, the values of the contact angles are elevated at all temperatures, but the ones on the lower temperature side become much larger. In other words, as the graft densities of PNIPA decrease, the changing of the contact angle of air bubble underneath the precisely prepared PNIPA-grafted membranes with temperature variation approaches that underneath the roughly prepared PNIPA brushes. From the FT-IR observation and the preparative condition, the decrease in the

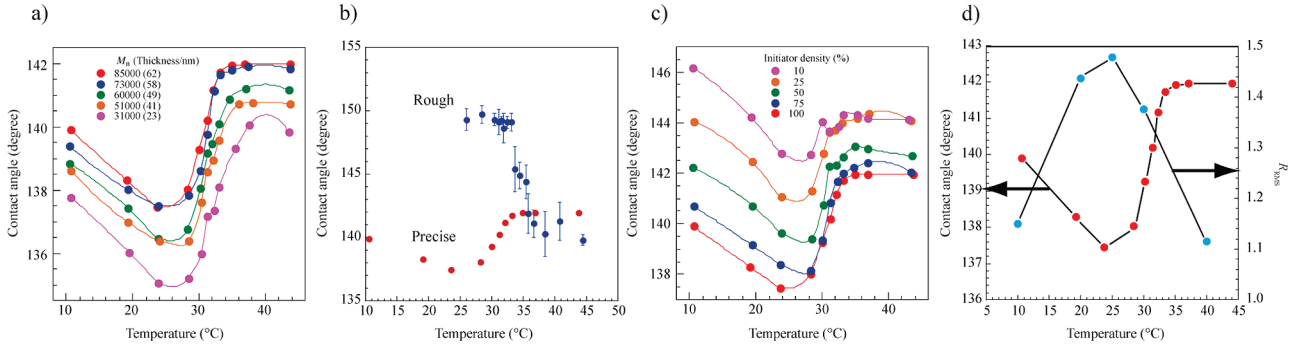

Figure 9. Contact angle of air bubble underneath PNIPA grafted membranes in water, (a) for the same high density PNIPA brushes with different molecular weight, (b) for the high density PNIPA brush with 85000 in M_n shown in part a compared with the roughly prepared PNIPA grafted brush (see Supporting Information, Figure S22), (c) for the almost same molecular weight PNIPA grafted membranes with different grafted densities, and (d) temperature dependent contact angle of air bubble underneath the high density PNIPA brush with 85 000 in M_n shown in part a is compared to the change in the surface roughness with changing temperature.

contact angle of the air bubble for the high-density PNIPA brushes at lower temperatures may be attributed to the decrease in the hydration ability of the polymer chains even in the vicinity of the surfaces and also the localization of the alkyl chloride end groups of the grafted PNIPA to the surface of the grafted membrane due to the stretched state of the grafted PNIPA. As, however, the contact angle of the air bubble underneath the monolayer composed of CPU−dMCS is 115° at 25 °C in water, the density of the alkyl chloride end groups is on the decline on the surface of the grafted membranes.

The most important parameters controlling wettability are the surface roughness, the relative area contributions of the chemically different portions of the surface, and their respective surface energies. If the surface is composed of single component rough surface and the size of an air bubble is sufficiently larger than the roughness scale, the Wenzel equation, considering the roughness of a surface, can be applied in the following form:[64]

$$\cos\theta = r\cos\theta_Y \tag{4}$$

where r is the roughness factor, which is the ratio of the actual and projected surface areas, and θ_Y is the Young contact angle (i.e., the intrinsic contact angle as calculated from Young's equation[76]). The value of r is always greater than 1. This equation states that the presence of roughness makes a hydrophilic surface more hydrophilic and a hydrophobic surface more hydrophobic than a flat surface with the same chemical composition. Since the values of θ in our system are larger than 90° at any temperature and the surfaces are categorized as hydrophilic surfaces, the increment in the roughness factor intensifies the values of θ. To examine the change in the surface roughness of the precisely prepared high-density PNIPA brush, the values of R_{rms} for the samples in water were measured by AFM at different temperatures. Figure 9d shows the temperature-dependent change in R_{rms} for sample No. 5′ and compares it with the equilibrium contact angles of air bubbles underneath the sample in water resulting from temperature changes. The temperature dependence for the values of R_{rms} shows a maximum at about 25 °C, whereas the values of θ with changes in temperature show a minimum at about 25 °C. Considering that the fluctuation of the polymer densities in solution systems and gel systems increases near the LCST, the maximum value of R_{rms} at about 25 °C must be attributed to maximizing the fluctuation of polymer densities in the brush.[77,78] If we applied the Wenzel equation to explain the change in θ with the variation of R_{rms}, the temperature dependence for the values of θ would also show a maximum at about 25 °C. However, just the opposite change occurred in our systems.

As the conformation of grafted polymers can change in the membrane due to temperature changes, the chemical composition on the surface of the membrane may also change because it is significantly influenced by the change in the interaction between polymers.[79] For this reason, we have to consider changes in chemical composition on the surface of the membrane with changes in temperature. If the surface is chemically heterogeneous with roughness, the Cassie equation is modified to account for the real contact areas between the bubble and the surface.[64] For a two-component surface, the roughness of both components of the surface can be considered by introducing the parameter r_i to describe the respective ratios between the real area of the rough surface divided by the projected two-dimensional areas.[80]

$$\cos\theta = r_1 f_1/(r_1 f_1 + r_2 f_2)\cos\theta_1 + r_2 f_2/(r_1 f_1 + r_2 f_2)\cos\theta_2 \tag{5}$$

The nature of the terminal groups of the elongated polymers significantly affects the contact angle of the surface of the PNIPA brushes. As the polymer chains are flexible even in the condensed brush state, the end groups of the grafted chains can move near the surfaces. The results for the temperature-dependent contact angles may be interpreted by assuming that the terminally chlorinated alkyl groups of the elongated polymers can be positioned on the surfaces or can be hidden in the vicinity of the membranes, depending on temperature. If the chemical compositions on the surfaces can be varied by changing the temperature and more than two components participate in the variation, the theoretical explanation should be more complicated due to a variety of factors. At present, because detailed experimental information on the chemical compositions of water surfaces as the temperature varies had not been available, we cannot verify the hypotheses. Moreover, because the displacement of the end groups to more hydrophilic or hydrophobic groups can be achieved for this polymer, the contribution of end groups to this characteristic change in the contact angle must be elucidated. Studies to confirm these hypotheses are being performed.

Conclusions

High-density thermo-sensitive PNIPA brushes can be successfully prepared under carefully controlled conditions. We have performed a systematic study of the physicochemical properties of the brushes. The gradual decrease in the thickness of the densely grafted brushes with temperature was assessed by AFM in water. In general, grafted membranes and gels have both high

swelling and high shrinking abilities that result in abrupt changes in thickness. Meanwhile, comparing the fully collapsed thickness with the dried thickness, we observed a significant interaction between PNIPA chains and water molecules in the brush, even in the fully collapsed state in water at 36 °C. In addition, FT-IR data indicate that the PNIPA chains in the brush behave partially like a collapsed state even at a sufficiently low temperature, e.g., at 15.2 °C in water. As above, the PNIPA chains in the high-density brush are in a physically constrained state and cannot fully interact with water at low temperatures, but they can interact with a greater amount of water at high temperatures. As a result, the thickness of the brush changes continuously over a much broader range with changes in temperature. Furthermore, the contact angle of air bubble underneath the high-density polymer brush also gradually decreases up to around 25 °C in water, indicating that the hydrophilicity of the surface decreases like the typical PNIPA grafted membranes and gels. However, the value of the contact angle starts to increase dramatically from around the LCST of free PNIPA in water and becomes constant over 40 °C. Eventually, the surface above 40 °C exhibits a more hydrophilic nature than that below the LCST. This temperature-dependent contact angle may be understood by assuming that the terminally chlorinated alkyl groups of the elongated PNIPAs can be positioned on the surfaces or hidden in the vicinity of the membranes, depending on the temperature.

Acknowledgment. Y.T. gratefully acknowledges the financial support of a Grant-in-Aid for Scientific Research from the Ministry of Education, Culture, Sports, Science, and Technology, Japan. NIPA was kindly provided by Kohjin Co., Ltd. We are also grateful to Prof. Maeda of Fukui University for helpful discussions and suggestions, to Prof. Katsumoto of Hiroshima University for his help with the interpretation of FT-IR spectra, and to Prof. Kawaguchi of Nagoya University for the measurement of bulk density of PNIPA.

Supporting Information Available: Text briefly describing the information presents, figures showing the synthetic route for [11-(2-bromo-2- methyl)propionyloxy]undecyldimethylchlorosilane, PNIPA, CPU−dMCS, MPU−dMCS, PNIPA grafted membrane, ^{1}H NMR spectra, contact angle of water on the BMPU−dMCS modified surface, XPS spectra and plots, AFM and photo images of memberanes, changes in static water contact angle and XPS peak area with reaction time, chemical structures of NIPA, PMDETA, and Me_6TREN, synthetic route of PNIPA grafted membrane, film thickness as a function of reaction time, solvent composition, and initiator density, phase transition temperatures, FT-IR spectra, illustration of the captive bubble method, contact angle of air bubble, structure and cross-sectional image of FT-IR cell, baseline-subtracted amide I band of linear PNIPA, and evolution of area ratio of high wavenumber component of amide I band of linear PNIPA in D_2O as a function of temperature, and tables of synthesis results, vibrational assignments, and polymerization results. This material is available free of charge via the Internet at http://pubs.acs.org.

References and Notes

(1) Stuart, M. A. C.; Huck, W. T. S.; Genzer, J.; Muller, M.; Ober, C.; Stamm, M.; Sukhorukov, G. B.; Szleifer, I.; Tsukruk, V. V.; Urban, M.; Winnik, F.; Zauscher, S.; Luzinov, I.; Minko, S. *Nat. Mater.* **2010**, *9* (2), 101–113.
(2) Ionov, L. *J. Mater. Chem.* **2010**, *20* (17), 3382–3390.
(3) Liu, F.; Urban, M. W. *Prog. Polym. Sci.* **2010**, *35* (1−2), 3–23.
(4) Luo, S. Z.; Xu, J.; Zhu, Z. Y.; Wu, C.; Liu, S. Y. *J. Phys. Chem. B* **2006**, *110* (18), 9132–9139.
(5) He, Y. Y.; Lodge, T. P. *Chem. Commun.* **2007**, *26*, 2732–2734.
(6) Nagase, K.; Kobayashi, J.; Kikuchi, A. I.; Akiyama, Y.; Kanazawa, H.; Okano, T. *Langmuir* **2008**, *24* (2), 511–517.
(7) Yoshida, R.; Uchida, K.; Kaneko, Y.; Sakai, K.; Kikuchi, A.; Sakurai, Y.; Okano, T. *Nature* **1995**, *374* (6519), 240–242.
(8) Oya, T.; Enoki, T.; Grosberg, A. Y.; Masamune, S.; Sakiyama, T.; Takeoka, Y.; Tanaka, K.; Wang, G. Q.; Yilmaz, Y.; Feld, M. S.; Dasari, R.; Tanaka, T. *Science* **1999**, *286* (5444), 1543–1545.
(9) Kim, S. W.; Bae, Y. H.; Okano, T. *Pharm. Res.* **1992**, *9* (3), 283–290.
(10) Feil, H.; Bae, Y. H.; Feijen, J.; Kim, S. W. *Macromolecules* **1993**, *26* (10), 2496–2500.
(11) Brannonpeppas, L.; Peppas, N. A. *J. Controlled Release* **1989**, *8* (3), 267–274.
(12) Miura, M.; Cole, C. A.; Monji, N.; Hoffman, A. S. *J. Biomater. Sci., Polym. Ed.* **1994**, *5* (6), 555–568.
(13) Hoffman, A. S. *Adv. Drug Delivery Rev.* **2002**, *54* (1), 3–12.
(14) Nakayama, D.; Takeoka, Y.; Watanabe, M.; Kataoka, K. *Angew. Chem., Int. Ed.* **2003**, *42* (35), 4197–4200.
(15) Stayton, P. S.; Shimoboji, T.; Long, C.; Chilkoti, A.; Chen, G. H.; Harris, J. M.; Hoffman, A. S. *Nature* **1995**, *378* (6556), 472–474.
(16) Osada, Y.; Gong, J. P. *Prog. Polym. Sci.* **1993**, *18* (2), 187–226.
(17) Wang, G. Q.; Kuroda, K.; Enoki, T.; Grosberg, A.; Masamune, S.; Oya, T.; Takeoka, Y.; Tanaka, T. *Proc. Natl. Acad. Sci. U.S.A.* **2000**, *97* (18), 9861–9864.
(18) Hirokawa, Y.; Tanaka, T. *J. Chem. Phys.* **1984**, *81* (12), 6379–6380.
(19) Alvarez-Lorenzo, C.; Guney, O.; Oya, T.; Sakai, Y.; Kobayashi, M.; Enoki, T.; Takeoka, Y.; Ishibashi, T.; Kuroda, K.; Tanaka, K.; Wang, G. Q.; Grosberg, A. Y.; Masamune, S.; Tanaka, T. *Macromolecules* **2000**, *33* (23), 8693–8697.
(20) Takeoka, Y.; Honda, M.; Seki, T.; Ishii, M.; Nakamura, H. *ACS Appl. Mater. Interfaces* **2009**, *1* (5), 982–986.
(21) Takeoka, Y.; Berker, A. N.; Du, R.; Enoki, T.; Grosberg, A.; Kardar, M.; Oya, T.; Tanaka, K.; Wang, G. Q.; Yu, X. H.; Tanaka, T. *Phys. Rev. Lett.* **1999**, *82* (24), 4863–4865.
(22) Kato, M.; Kamigaito, M.; Sawamoto, M.; Higashimura, T. *Macromolecules* **1995**, *28* (5), 1721–1723.
(23) Wang, J. S.; Matyjaszewski, K. *Macromolecules* **1995**, *28* (23), 7901–7910.
(24) Ejaz, M.; Yamamoto, S.; Ohno, K.; Tsujii, Y.; Fukuda, T. *Macromolecules* **1998**, *31* (17), 5934–5936.
(25) Ohno, K.; Morinaga, T.; Koh, K.; Tsujii, Y.; Fukuda, T. *Macromolecules* **2005**, *38* (6), 2137–2142.
(26) de Gennes, P. G. *Nobel Lecture*, December 9. **1991**.
(27) Okano, T.; Yamada, N.; Sakai, H.; Sakurai, Y. *J. Biomed. Mater. Res.* **1993**, *27* (10), 1243–1251.
(28) Zhang, J.; Pelton, R.; Deng, Y. L. *Langmuir* **1995**, *11* (6), 2301–2302.
(29) Nakamura, T.; Hattori, M.; Kawasaki, H.; Miyamoto, K.; Tokita, M.; Komai, T. *Phys. Rev. E* **1996**, *54* (2), 1663–1668.
(30) Ito, Y.; Chen, G. P.; Guan, Y. Q.; Imanishi, Y. *Langmuir* **1997**, *13* (10), 2756–2759.
(31) Liang, L.; Rieke, P. C.; Fryxell, G. E.; Liu, J.; Engehard, M. H.; Alford, K. L. *J. Phys. Chem. B* **2000**, *104* (49), 11667–11673.
(32) Bao, Z. Y.; Bruening, M. L.; Baker, G. L. *Macromolecules* **2006**, *39* (16), 5251–5258.
(33) Matyjaszewski, K.; Miller, P. J.; Shukla, N.; Immaraporn, B.; Gelman, A.; Luokala, B. B.; Siclovan, T. M.; Kickelbick, G.; Vallant, T.; Hoffmann, H.; Pakula, T. *Macromolecules* **1999**, *32* (26), 8716–8724.
(34) Yamamoto, S.; Ejaz, M.; Tsujii, Y.; Fukuda, T. *Macromolecules* **2000**, *33* (15), 5608–5612.
(35) Yamamoto, S.; Ejaz, M.; Tsujii, Y.; Matsumoto, M.; Fukuda, T. *Macromolecules* **2000**, *33* (15), 5602–5607.
(36) Advincula, R.; Brittain, W. J.; Caster, K. C.; Rühe, J., Ed., *Polymer Brushes: Synthesis, Characterization, Applications*; Wiley-VCH: Weinheim, Germany, 2004.
(37) Jones, D. M.; Smith, J. R.; Huck, W. T. S.; Alexander, C. *Adv. Mater.* **2002**, *14* (16), 1130–1134.
(38) Balamurugan, S.; Mendez, S.; Balamurugan, S. S.; O'Brien, M. J.; Lopez, G. P. *Langmuir* **2003**, *19* (7), 2545–2549.
(39) Kaholek, M.; Lee, W. K.; Ahn, S. J.; Ma, H. W.; Caster, K. C.; LaMattina, B.; Zauscher, S. *Chem. Mater.* **2004**, *16* (19), 3688–3696.
(40) Tu, H. L.; Hong, L.; Anthony, S. M.; Braun, P. V.; Granick, S. *Langmuir* **2007**, *23* (5), 2322–2325.
(41) Yim, H.; Kent, M. S.; Satija, S.; Mendez, S.; Balamurugan, S. S.; Balamurugan, S.; Lopez, G. P. *Phys. Rev. E* **2005**, *72* (5).
(42) Liu, Y.; Klep, V.; Luzinov, I. *J. Am. Chem. Soc.* **2006**, *128* (25), 8106–8107.
(43) Plunkett, K. N.; Zhu, X.; Moore, J. S.; Leckband, D. E. *Langmuir* **2006**, *22* (9), 4259–4266.

(44) Lokuge, I.; Wang, X.; Bohn, P. W. *Langmuir* **2007**, *23* (1), 305–311.
(45) He, Q.; Kuller, A.; Grunze, M.; Li, J. B. *Langmuir* **2007**, *23* (7), 3981–3987.
(46) Schepelina, O.; Zharov, I. *Langmuir* **2007**, *23* (25), 12704–12709.
(47) Mathieu, M.; Friebe, A.; Franzka, S.; Ulbricht, M.; Hartmann, N. *Langmuir* **2009**, *25* (20), 12393–12398.
(48) Wang, S. Q.; Zhu, Y. X. *Langmuir* **2009**, *25* (23), 13448–13455.
(49) Teodorescu, M.; Matyjaszewski, K. *Macromolecules* **1999**, *32* (15), 4826–4831.
(50) Rademacher, J. T.; Baum, R.; Pallack, M. E.; Brittain, W. J.; Simonsick, W. J. *Macromolecules* **2000**, *33* (2), 284–288.
(51) Bontempo, D.; Li, R. C.; Ly, T.; Brubaker, C. E.; Maynard, H. D. *Chem. Commun.* **2005**, No. 37, 4702–4704.
(52) Xu, J.; Ye, J.; Liu, S. Y. *Macromolecules* **2007**, *40* (25), 9103–9110.
(53) Masci, G.; Giacomelli, L.; Crescenzi, V. *Macromol. Rapid Commun.* **2004**, *25* (4), 559–564.
(54) Millard, P.-E.; Mougin, N. C.; Böker, A.; Müller, A. H. E. *Controlled/Living Radical Polymerization: Progress in ATRP*; Matyjaszewski, K., Ed.; ACS Symposum Series; American Chemical Society: Washington, DC, 2009; pp 127−137.
(55) Jonas, A. M.; Glinel, K.; Oren, R.; Nysten, B.; Huck, W. T. S. *Macromolecules* **2007**, *40* (13), 4403–4405.
(56) Fadeev, A. Y.; McCarthy, T. J. *Langmuir* **2000**, *16* (18), 7268–7274.
(57) Fadeev, A. Y.; McCarthy, T. J. *Langmuir* **1999**, *15* (11), 3759–3766.
(58) Tong, Q. Y.; Gosele, U. M. *Adv. Mater.* **1999**, *11* (17), 1409–1425.
(59) Donose, B. C.; Taran, E.; Vakarelski, I. U.; Shinto, H.; Higashitani, K. *J. Colloid Interface Sci.* **2006**, *299* (1), 233–237.
(60) Armistea, Cg; Tyler, A. J.; Hambleto, Fh; Mitchell, S. A.; Hockey, J. A. *J. Phys. Chem.* **1969**, *73* (11), 3947–3953.
(61) Zhuravlev, L. T. *Langmuir* **1987**, *3* (3), 316–318.
(62) Jones, D. M.; Brown, A. A.; Huck, W. T. S. *Langmuir* **2002**, *18* (4), 1265–1269.
(63) Wang, X. J.; Tu, H. L.; Braun, P. V.; Bohn, P. W. *Langmuir* **2006**, *22* (2), 817–823.
(64) Marmur, A. *Soft Matter* **2006**, *2* (1), 12–17.
(65) Israelachvili, J. N.; Gee, M. L. *Langmuir* **1989**, *5* (1), 288–289.
(66) Fukuda, T.: Tsujii, Y.; Ohno, K.; *Macromolecular Engineering. Precise Synthesis, Materials Properties, Applications*; Matyjaszewski, K., Gnanou, Y., Leibler, L., Eds.; Wiley-VCH: Weinheim, Germany, 2007.
(67) Shah, R. R.; Merreceyes, D.; Husemann, M.; Rees, I.; Abbott, N. L.; Hawker, C. J.; Hedrick, J. L. *Macromolecules* **2000**, *33* (2), 597–605.
(68) Zhulina, E. B.; Borisov, O. V.; Pryamitsyn, V. A.; Birshtein, T. M. *Macromolecules* **1991**, *24* (1), 140–149.
(69) Maeda, Y.; Higuchi, T.; Ikeda, I. *Langmuir* **2000**, *16* (19), 7503–7509.
(70) Katsumoto, Y.; Tanaka, T.; Sato, H.; Ozaki, Y. *J. Phys. Chem. A* **2002**, *106* (14), 3429–3435.
(71) Ahmed, Z.; Gooding, E. A.; Pimenov, K. V.; Wang, L. L.; Asher, S. A. *J. Phys. Chem. B* **2009**, *113* (13), 4248–4256.
(72) Hu, T. J.; You, Y. Z.; Pan, C. Y.; Wu, C. *J. Phys. Chem. B* **2002**, *106* (26), 6659–6662.
(73) Suzuki, A.; Kobiki, Y. *Jpn. J. Appl. Phys., Part 1: Reg. Pap. Short Notes Rev. Pap.* **1999**, *38* (5A), 2910–2916.
(74) Takeoka, Y.; Watanabe, M. *Langmuir* **2002**, *18* (16), 5977–5980.
(75) Jonas, A. M.; Hu, Z. J.; Glinel, K.; Huck, W. T. S. *Nano Lett.* **2008**, *8* (11), 3819–3824.
(76) The Young equation, $\cos\theta = (\sigma_{sf} - \sigma_{sl})/\sigma_{lf,}$ was developed in the case of an ideal solid surface, which is defined as smooth, rigid, chemically homogeneous, insoluble, and nonreactive.
(77) Tanaka, T. *Sci. Am.* **1981**, *244*, 124–136.
(78) Laloyaux, X.; Mathy, B.; Nysten, B.; Jonas, A. M. *Langmuir* **2010**, *26* (2), 838–847.
(79) Senshu, K.; Yamashita, S.; Ito, M.; Hirao, A.; Nakahama, S. *Langmuir* **1995**, *11* (6), 2293–2300.
(80) Järn, M.; Brieler, F. J.; Kuemmel, M.; Grosso, D.; Linden, M. *Chem. Mater.* **2008**, *20* (4), 1476–1483.